

# Structure, Magnetic Properties, and Magnetoimpedance of the $\text{Fe}_{73.5-x}\text{Cr}_x\text{Si}_{13.5}\text{B}_9\text{Nb}_3\text{Cu}_1$ ( $x = 0$ to 5) Alloys

Stanislav O. Volchkov<sup>1</sup>, Vera A. Lukshina<sup>2</sup>, Anna A. Zakharova<sup>1,2</sup>, Alexander P. Potapov<sup>2</sup>, and Elena G. Volkova<sup>2</sup>

<sup>1</sup>Ural Federal University, Ekaterinburg 620002, Russia

<sup>2</sup>Ural Division, Russian Academy of Sciences, Institute of Metal Physics, Ekaterinburg 620990, Russia

**Structure, magnetic properties, and magnetoimpedance (MI) of the nanocrystalline  $\text{Fe}_{73.5-x}\text{Cr}_x\text{Si}_{13.5}\text{B}_9\text{Nb}_3\text{Cu}_1$  ( $x = 0\%$ ,  $1\%$ ,  $2\%$ ,  $3\%$ , and  $5\%$ ) ribbons produced by rapid quenching after thermal annealing at  $520^\circ\text{C}$  for 2 h were investigated with the aim to produce materials with different functional possibilities. It was shown that increasing the Cr content to  $5\%$  leads to a large increase of the coercivity of the samples due to phases  $\text{Fe}_2\text{B}$  and Cr appearing together with a drastic increase of the surface roughness. The possibility of determination of volume of these non-homogeneous was presented by a method based on MI effect. It was shown that the addition of Cr not only increased the MI effect, but also the peak of MI is shifted to the higher fields. It can be used for magnetic field sensors in certain ranges of magnetic fields.**

**Index Terms**—Fe-based nanocrystalline alloys, magnetic properties, magnetoimpedance (MI).

## I. INTRODUCTION

THE study of the structure and magnetic properties of nanocrystalline  $\text{FeSiNbCu}$  alloys is an important research and applications line [1], [2]. These materials have record magnetic permeability and high values of the magnetoimpedance (MI) effect, they are characterized by unusual structural, electrical, magnetic, optical properties, and their resistance to corrosion [3]–[8]. New alloys based on the classic [1]  $\text{Fe}_{73.5}\text{Si}_{13.5}\text{B}_9\text{Nb}_3\text{Cu}_1$  composition are under development (via slight variation of the composition) aiming to obtain enhanced functional properties. It was shown [5]–[7] that Cr addition and Fe reduction, compared with the classic composition increase the crystallization temperature and the resistance to corrosion of the alloys.

An interest to the MI in this paper is explained not only the capabilities for the applications for detecting a weak magnetic fields, but also as a method to study the features of the magnetic anisotropy and the structural state of the tested materials, which cannot be detected on magnetostatic studies [8]–[10].

## II. EXPERIMENTAL

In this paper, amorphous  $\text{Fe}_{73.5-x}\text{Cr}_x\text{Si}_{13.5}\text{B}_9\text{Nb}_3\text{Cu}_1$  ( $x = 0\%$ ,  $1\%$ ,  $2\%$ ,  $3\%$ , and  $5\%$ ) alloys were obtained by rapid quenching from the melt. The concentration of Cr has been controlled during the preparation of the samples by weight. Annealing for 2 h at the temperature of  $520^\circ\text{C}$  led to nanocrystallization. The structural state was investigated by transmission electron microscopy (TEM) on an SM 300 microscope. Magnetic properties were studied by the ballistic method using galvanometric compensation

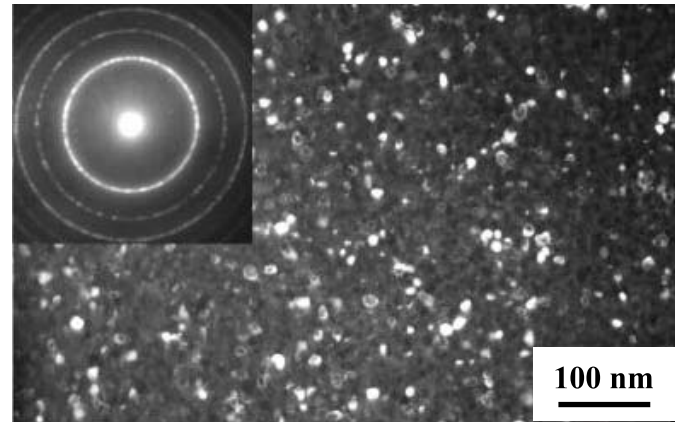


Fig. 1. Dark-field image and electron diffraction pattern for specimen with 1% Cr content.

microfluxmeter, samples ( $20\ \mu\text{m} \times 1\ \text{mm} \times 100\ \text{mm}$ ) were magnetized and hysteresis loops were measured along the ribbon axis.

The longitudinal MI, i.e., MI for external in-plain magnetic field is parallel to the ribbon axis and to the direction of the driving alternating current, was measured in the microstrip line for amplitude of the sinusoidal current  $I_{\text{rms}} = 10\ \text{mA}$ , in a frequency range of 1–200 MHz. The MI was measured in fully automated system using Agilent HP e4991A Analyser. The relative values of the total impedance ( $Z$ ) were calculated as follows:  $\Delta Z/Z = 100 \times (Z(H) - Z(H_{\max})/Z(H_{\max}))$ , where  $H_{\max} = 100\ \text{Oe}$ . All measurements were done at room temperature.

## III. RESULTS AND DISCUSSION

The structural investigation of alloys shows that the alloys contain mainly grains (10–12 nm in size) of solid solution with the rest of amorphous phase along grain boundaries. Figs. 1 and 2 show TEM data for  $\text{Fe}_{73.5}\text{Si}_{13.5}\text{B}_9\text{Nb}_3\text{Cu}_1$  and  $\text{Fe}_{68.5}\text{Cr}_5\text{Si}_{13.5}\text{B}_9\text{Nb}_3\text{Cu}_1$  nanocrystalline alloys, respectively.

Manuscript received March 8, 2014; revised April 17, 2014; accepted May 1, 2014. Date of current version November 18, 2014. Corresponding author: S. O. Volchkov (e-mail: stanislav.volchkov@urfu.ru).

Color versions of one or more of the figures in this paper are available online at <http://ieeexplore.ieee.org>.

Digital Object Identifier 10.1109/TMAG.2014.2335416

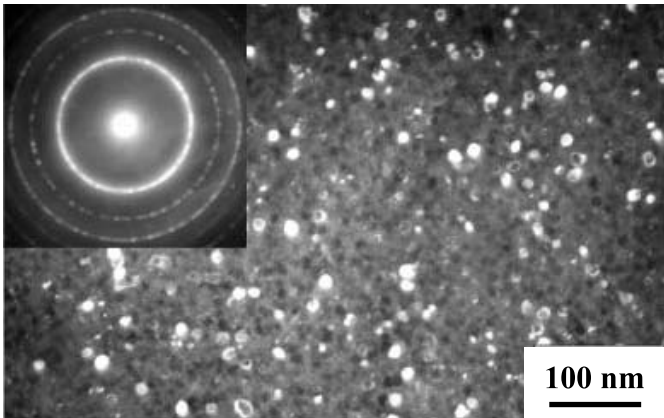


Fig. 2. Dark-field image and electron diffraction pattern for specimen with 5% Cr content.

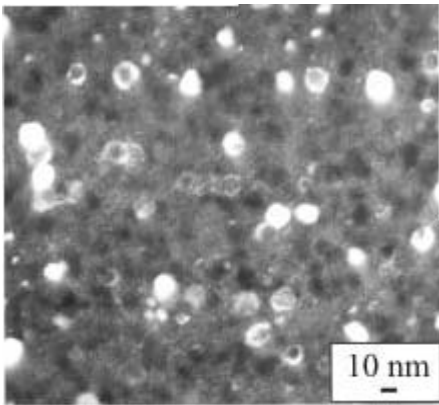


Fig. 3. Dark-field image of specimen with 5% Cr content.

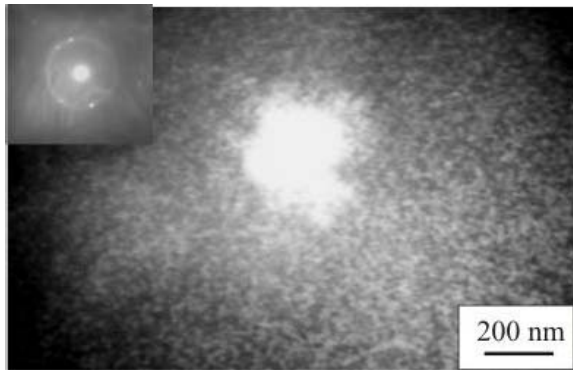


Fig. 4. Bright-field image of individual large bcc particle and electron diffraction pattern.

The microdiffraction pictures show faint lines of  $\text{Fe}_3\text{Si}$  phase, individual reflexes of  $\text{Fe}_2\text{B}$  and oxides of iron. The study of the structure did not show any difference in both average grain size and phases composition for alloys with different Cr content. Nevertheless, for alloys with 3% and 5% Cr dark-field images show large number of grains with size of 1–2 nm (Fig. 3, for 5% Cr). It can be precipitates of Cr or nuclei of solid solution. In addition, all specimens had a few number of big grains of solid solution with size up to 200 nm (Fig. 4).

Fig. 6 shows the quasi-static magnetic hysteresis loop for samples  $\text{Fe}_{73.5-x}\text{Cr}_x\text{Si}_{13.5}\text{B}_9\text{Nb}_3\text{Cu}_1$  ( $x = 0\%, 1\%, 2\%, 3\%$ , and  $5\%$ ). Table I shows the main magnetic properties of the samples.

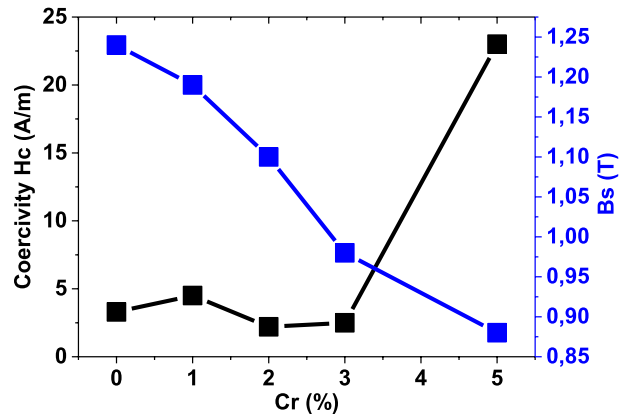


Fig. 5. Magnetic characteristics of the samples  $\text{Fe}_{73.5-x}\text{Cr}_x\text{Si}_{13.5}\text{B}_9\text{Nb}_3\text{Cu}_1$  ( $x = 0\%, 1\%, 2\%, 3\%$ , and  $5\%$ ).

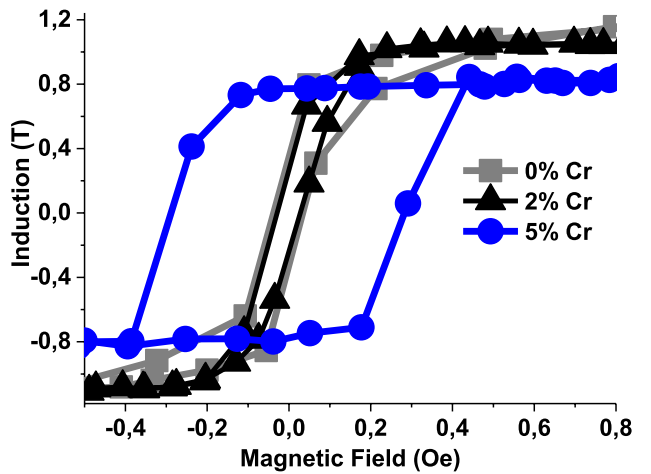


Fig. 6. Quasi-static magnetic hysteresis loop for samples  $\text{Fe}_{73.5-x}\text{Cr}_x\text{Si}_{13.5}\text{B}_9\text{Nb}_3\text{Cu}_1$  ( $x = 0\%, 1\%, 2\%, 3\%$ , and  $5\%$ ). Bs—SATURATION MAGNETIC INDUCTION, Hc—COERCIVITY, AND L—DIMENSION OF ROUGHNESS

TABLE I

MAGNETIC CHARACTERISTICS OF THE SAMPLES  
 $\text{Fe}_{73.5-x}\text{Cr}_x\text{Si}_{13.5}\text{B}_9\text{Nb}_3\text{Cu}_1$  ( $x = 0\%, 1\%, 2\%, 3\%$ ,  
 AND  $5\%$ ). Bs—SATURATION MAGNETIC  
 INDUCTION, Hc—COERCIVITY, AND  
 L—DIMENSION OF ROUGHNESS

Cr, %	Bs (T)	Hc (A/m)	L ( $\mu\text{m}$ )
0	1.24	3.3	156
1	1.19	4.5	129
2	1.10	2.2	140
3	0.98	2.5	133
5	0.88	23	198

The form of hysteresis loops indicates that the material has soft magnetic properties with in-plane anisotropy with the easy magnetization axis oriented along the long side of the samples, without the presence of additional contributions (e.g., local stresses) that may occur during the manufacturing process. This is explained by fact that during the annealing phase appears  $\text{Fe}_3\text{Si}$ , which improves the soft magnetic properties, because of the strong exchange interaction between the magnetic grains. The saturation induction decreases with additive increasing of content of Cr in the alloy from the substitution

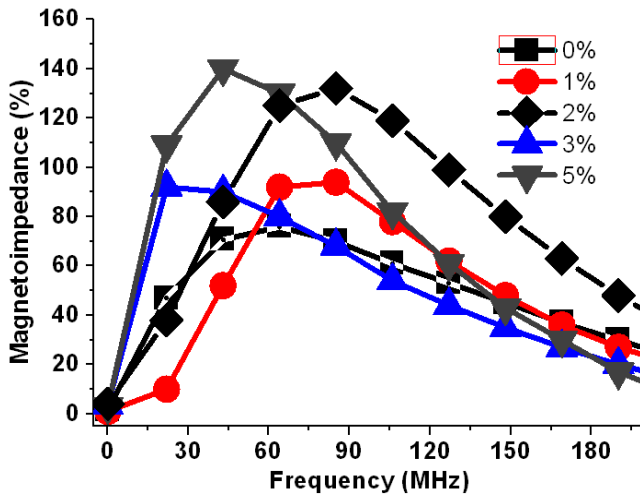


Fig. 7. Frequency dependences of MI for samples with Cr (0%, 1%, 2%, 3%, and 5%).

of magnetic Fe by non-magnetic Cr. The saturation induction was gradually decreased from 1.24 T for classic composition to about 0.88 T for  $\text{Fe}_{68.5}\text{Cr}_5\text{Si}_{13.5}\text{B}_9\text{Nb}_3\text{Cu}_1$  composition. Coercivity does not show the linear. The samples, which are containing Cr = 2% and 3% shows the lowest coercivity. This is explained by fact that in the process of the formation of nanocrystallites  $\text{Fe}_3\text{Si}$  are optimal conditions, which reduces the magnetostriction constant and hence the magnetoelastic anisotropy. We note that the process of nanocrystallization begins in the surface region and then spreads to over the entire volume of the sample.

The formation of ultrafine nanograins  $\text{Fe}_3\text{Si}$  with grain size (10–12 nm), wherein the magnetocrystalline anisotropy is averaged out and there is a strong exchange interaction, is resulting to higher soft magnetic properties. A further increase of the boride phases  $\text{Fe}_2\text{B}$ , which have a high-magnetic anisotropy, resulting in an increase in coercive force and an increase of roughness. Microscopic studies of sample with Cr = 5% showed that the smaller clusters (1–2 nm) of chromium, or a new phase embryos are appeared and they have also contributed to the increase in coercivity. Thus, strong magnetoanizotropy effect of iron  $\text{Fe}_2\text{B}$  and Cr together with a sharp increase in the roughness of the surface profile, which prevents smooth movement of the domain wall, are deteriorated of soft magnetic properties.

Fig. 7 shows dependences of MI  $\Delta Z/Z$  for samples  $\text{Fe}_{73.5-x}\text{Cr}_x\text{Si}_{13.5}\text{B}_9\text{Nb}_3\text{Cu}_1$  ( $x = 0\%$ , 1%, 3%, and 5%) after nanocrystallization, depending on the frequency of the current.

Values for all the samples have a characteristic maximum ( $\Delta Z/Z = 74\%$  for Cr = 0%,  $\Delta Z/Z = 140\%$  for Cr = 5%) in the frequency range from 24 to 106 MHz. In the low-frequency changing of impedance due to, mainly, a conventional frequency-dependent phase shift between the current and the probe voltage, a current flows through the entire sample volume. Maximum frequency becomes that threshold, when the skin depth is compared with the value of the order of the thickness of the zone of non-homogeneity easy magnetization axes in the surface layer due to the presence of hard magnetic phases or structural inhomogeneities.

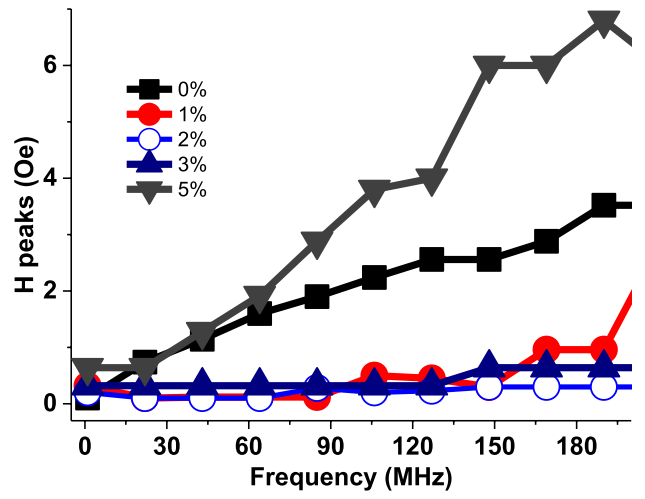


Fig. 8. Frequency dependences of MI peaks on magnetic field scale for samples with Cr (0%, 1%, 3%, and 5%).

Under such conditions the current distribution across the section, as well as processes and dynamic magnetization reversal, becomes non-uniform. In addition, when the frequency is increased in further is resulting in a decrease of the transverse magnetic susceptibility. The last fact is the reason for reducing the value of the magneto impedance. The differences in this threshold value indicate the difference in the volume zone of non-homogeneity of easy magnetization axes of the various samples in the surface zone. In addition, in the high-frequency range ( $f > 100$  MHz) domain wall motion is strongly damped by eddy currents, which contributes to reduction of the transverse magnetic permeability is responsible for the effect of MI.

Fig. 8 shows the dependence of the external magnetic field (Hpeaks) at which the maximum MI is fixed from the current current. For example, in the sample containing Cr = 0% at the frequency 85 MHz the peak appears in the Hpeaks = 1.9 Oe and at the same frequency when the content of Cr = 1%, 2%, and 3%, the peak appears in the Hpeaks = 0, 32 Oe. The increasing of the Cr-content to 5% leads to a displacement of the peak GMI to higher fields ( $H = 2.8$  Oe). These results are fully correlated with changes in the structural and magnetic characteristics (Table I and Fig. 5). The appearance of additional magnetically hard phases in the sample with Cr = 5% make the dynamic magnetization reversal difficult. It may also affect the average size of local structural non-homogeneities in the sample and, as a consequence, modify the process of movement of the domain walls. The ac field generated by the current may increase the energy of domain walls and distortion. In this case, MI response may depend on the size of the non-homogeneities in the case of irregularities, comparable with the width of the domain wall. The observed peaks with different features on the scale of the magnetic field can be used in applications requiring high sensitivity in a certain area of the magnetic field.

Fig. 9 shows the field dependence of the MI at various frequencies for the samples containing Cr = 1% and 5%. These data also correlate completely with the variation of structural and magnetic characteristics (Table I). In the case

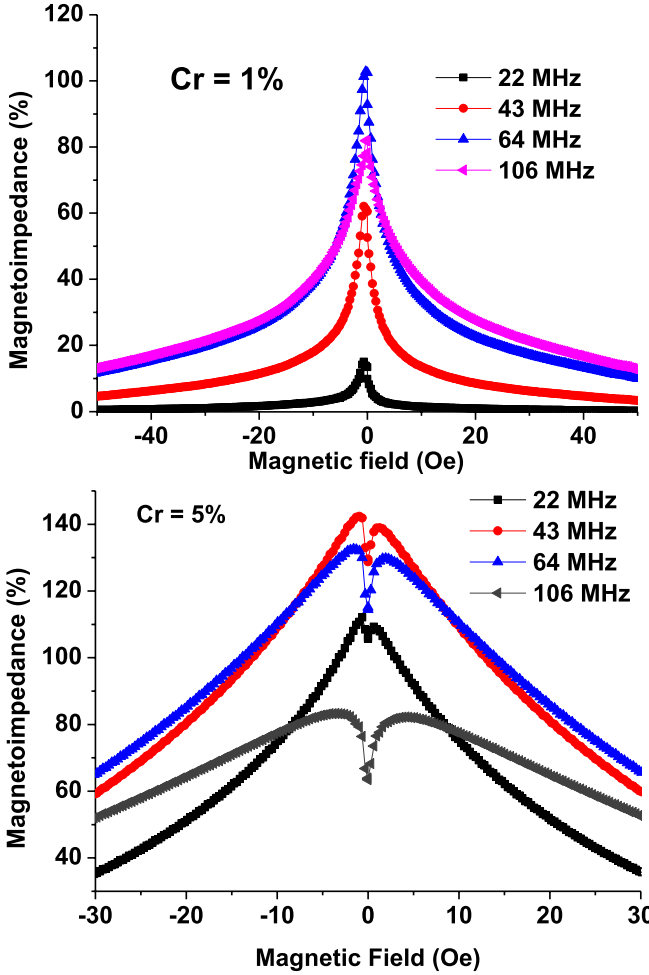


Fig. 9. Field MI-dependences for sample with 1% and 5% Cr with different frequencies.

of 1%, 2%, and 3% we see the single peak structure for the all frequency range, which reveals a planar anisotropy with the easy axis oriented strictly along the long side of the sample, without the presence of additional contributions of non-homogeneities. In addition, in the case of 5% double-peaked structure with a dip in the small magnetic fields, which explains the appearance of a small fraction of the magnetic phase with non-longitudinal orientation of vectors of spontaneous magnetization. Such areas may be formed in the deposition phase of Fe<sub>3</sub>Si and Fe<sub>2</sub>B, which were resulting in higher Hc, or/and due to inhomogeneities or local structural characteristics of the surface roughness. Note, that dip is observed at all frequencies, which means a significant amount of magnetic inhomogeneity zone for the sample with Cr = 5%, and can be calculated from the model to the skin depth.

#### IV. CONCLUSION

Structure, magnetic properties, and MI of the nanocrystalline Fe<sub>73.5-x</sub>Cr<sub>x</sub>Si<sub>13.5</sub>B<sub>9</sub>Nb<sub>3</sub>Cu<sub>1</sub> ( $x = 0\%$ , 1%, 2%, 3%, and 5%) ribbons produced by rapid quenching after thermal annealing at 520 °C for 2 h were investigated.

It has been shown that increasing the Cr content to 5% leads to a large increase of the coercivity of the samples due to phases Fe<sub>2</sub>B and Cr appearing together with a drastic increase of the surface roughness. The possibility of determination of volume of these non-homogeneous was presented by method based on MI effect. It was shown, that the addition of Cr not only increases the MI effect, but the peak of MI is shifted to the higher fields. It can be used for magnetic field sensors in certain range of magnetic fields.

#### ACKNOWLEDGMENT

This work was supported in part by the Presidium of Russian Academy of Sciences under Project 12-II-23-2005 and in part by the Ministry of Education and Science of the Russian Federation under Contract 02.G36.31.0004.

#### REFERENCES

- [1] Y. Yoshizawa, S. Oguma, and K. Yamauchi, "New Fe-based soft magnetic alloys composed of ultrafine grain structure," *J. Appl. Phys.*, vol. 64, no. 10, pp. 6044–6046, 1988.
- [2] G. Herzer, *Encyclopedia of Materials: Science and Technology*. Amsterdam, The Netherlands: Elsevier, 2001.
- [3] A. S. Antonov *et al.*, *Fiz. Mater. Metalloved.*, vol. 83, no. 6, p. 61, 1997.
- [4] M. Vazquez *et al.*, "Frequency dependence of the magnetoimpedance in nanocrystalline FeCuNbSiB with high transverse stress-induced magnetic anisotropy," *IEEE Trans. Magn.*, vol. 35, no. 5, pp. 3358–3360, Sep. 1999.
- [5] N. Chau, P. Q. Thanh, N. Q. Hoa, and N. D. The, "The existence of giant magnetocaloric effect and laminar structure in Fe<sub>73.5-x</sub>Cr<sub>x</sub>Si<sub>13.5</sub>B<sub>9</sub>Nb<sub>3</sub>Cu<sub>1</sub>," *J. Magn. Magn. Mater.*, vol. 304, no. 1, pp. 36–40, 2006.
- [6] V. A. Lukshina, N. V. Dmitrieva, M. A. Cerdeira, and A. P. Potapov, "Stress-induced magnetic anisotropy in Fe-based nanocrystalline alloy with addition of 1–5 at.% Cr," *J. Alloys Compounds*, vol. 536, pp. S374–S376, Sep. 2012.
- [7] G. V. Kurlyandskaya, V. A. Lukshina, A. Larrañaga, I. Orue, A. A. Zaharova, and D. A. Shishkin, "Induced magnetic anisotropy features in FeCrSiBNbCu nanocrystalline alloy: Role of stress distribution proven by direct X-ray measurements," *J. Alloys Compounds*, vol. 566, pp. 31–36, Jul. 2013.
- [8] A. V. Semirov *et al.*, "Temperature dependences of magnetoimpedance of nanocrystalline Fe-based ribbons," *J. Nanosci. Nanotechnol.*, vol. 12, no. 9, pp. 7446–7450, 2012.
- [9] G. V. Kurlyandskaya *et al.*, "Magnetic properties and the magnetoimpedance effect of nanostructured Fe<sub>73.5</sub>Si<sub>16.5</sub>B<sub>6</sub>Nb<sub>3</sub>Cu<sub>1</sub> ribbons with induced magnetic anisotropy," *Bull. Russian Acad. Sci., Phys.*, vol. 74, no. 10, pp. 1466–1468, Oct. 2010.
- [10] A. V. Semirov, D. A. Bukreev, A. A. Moiseev, V. A. Lukshina, E. G. Volkova, and S. O. Volchkov, "Influence of the special features of the effective magnetic anisotropy on the temperature dependences of the magnetoimpedance of nanocrystalline Fe<sub>73.5</sub>Si<sub>16.5</sub>B<sub>6</sub>Nb<sub>3</sub>Cu<sub>1</sub> strips," *Russian Phys. J.*, vol. 54, no. 5, pp. 612–618, Oct. 2011.